Electrocatalytic Activity of Spots of Electrodeposited Noble-Metal Catalysts on Carbon Nanotubes Modified Glassy Carbon

5 AUTHORS, INCLUDING:

Xingxing Chen
Ruhr-Universität Bochum
26 PUBLICATIONS **436** CITATIONS

SEE PROFILE

Kathrin Eckhard
Hydro Aluminium
23 PUBLICATIONS **535** CITATIONS

SEE PROFILE

Min Zhou
University of Texas MD Anderson Cancer C…
45 PUBLICATIONS **1,150** CITATIONS

SEE PROFILE

Electrocatalytic Activity of Spots of Electrodeposited Noble-Metal Catalysts on Carbon Nanotubes Modified Glassy Carbon

Xingxing Chen, Kathrin Eckhard, Min Zhou, Michael Bron, and Wolfgang Schuhmann*

Analytische Chemie, Elektroanalytik & Sensorik, Ruhr-Universität Bochum, Universitätsstrasse 150, D-44780 Bochum, Germany

A strategy for the screening of the electrocatalytic activity of electrocatalysts for possible application in fuel cells and other devices is presented. In this approach, metal nanoclusters (Pt, Au, Ru, and Rh and their codeposits) were prepared using a capillary-based droplet-cell by pulsed electrodeposition in a diffusion-restricted viscous solution. A glassy carbon surface was modified with carbon nanotubes (CNTs) by electrophoretic accumulation and was used as substrate for metal nanoparticle deposition. The formed catalyst spots on the CNT-modified glassy carbon surface were investigated toward their catalytic activity for oxygen reduction as a test reaction employing the redox competition mode of scanning electrochemical microscopy (RC-SECM). Qualitative information on the electrocatalytic activity of the catalysts was obtained by varying the potential applied to the substrate; semiquantitative evaluation was based on the determination of the electrochemically deposited catalyst loading by means of the charge transferred during the metal nanoparticle deposition. Qualitatively, Au showed the highest electrocatalytic activity toward the oxygen reduction reaction (ORR) in phosphate buffer among all investigated single metal catalysts which was attributed to the much higher loading of Au achieved during electrodeposition. Coelectrodeposited Au−Pt catalysts showed a more positive onset potential (−150 mV in RC-SECM experiments) of the ORR in phosphate buffer at pH 6.7. After normalizing the SECM image by the charge during the metal nanocluster deposition which represents the mass loading of the catalyst, Ru showed a higher electrocatalytic activity toward the ORR than Au.

One topic of great interest in PEM (proton exchange membrane) fuel cell research over the last decades is the development of novel catalysts with low cost and high electrocatalytic activity.[1−4]

Carbon supported Pt and its alloys have been established as state of the art catalysts for anode and cathode reactions in PEM fuel cells.[5−9] Different routes such as impregnation/reduction, colloidal methods, spontaneous reduction, and electroless deposition have been developed to prepare highly dispersed catalysts with small particle size in order to efficiently use the precious metal.[10−15] Besides, electrochemical deposition, especially the pulsed electrodeposition technique,[6,16−18] is proving to be an increasingly attractive route for the preparation of catalyst nanoparticles due to its simple operation, high purity of deposits, and easy control of the particle size.[19] In the case of electrocatalysis, electrodeposition is especially attractive due to the fact that deposition takes place only at electrically connected sites.

Besides the active metal itself, the catalyst support is also playing an important role in achieving good electrode performance.[20] Carbon nanotubes (CNTs) are attracting growing interest in catalysis due to their combination of beneficial properties such as their relatively large surface area, advantageous chemical properties (e.g., stability), and especially their high electric conductivity,[21−24] making them also attractive for fuel cell ap-

(5) De Bruijn, F. *Green Chem.* **2005**, *7* (3), 132–150.
(6) Loffler, M. S.; Natter, H.; Hempelmann, R.; Wippermann, K. *Electrochim. Acta* **2003**, *48* (20−22), 3047–3051.
(7) Tripkovic, A. V.; Popovic, K. D.; Grgur, B. N.; Blizanac, B.; Ross, P. N.; Markovic, N. M. *Electrochim. Acta* **2002**, *47* (22−23), 3707–3714.
(8) Gotz, M.; Wendt, H. *Electrochim. Acta* **1998**, *43* (24), 3637–3644.
(9) Page, T.; Johnson, R.; Hormes, J.; Noding, S.; Rambabu, B. *J. Electroanal. Chem.* **2000**, *485* (1), 34–41.
(10) Puntes, V. F.; Krishnan, K. M.; Alivisatos, A. P. *Science* **2001**, *291* (5511), 2115–2117.
(11) Sun, Y. G.; Xia, Y. N. *Science* **2002**, *298* (5601), 2176–2179.
(12) Kong, J.; Chapline, M. G.; Dai, H. J. *Adv. Mater.* **2001**, *13* (18), 1384–1386.
(13) Lago, R. M.; Tsang, S. C.; Lu, K. L.; Chen, Y. K.; Green, M. L. H. *Chem. Commun.* **1995**, (13), 1355–1356.
(14) Liu, Z. L.; Ling, X. Y.; Su, X. D.; Lee, J. Y. *J. Phys. Chem. B* **2004**, *108* (24), 8234–8240.
(15) Choi, H. C.; Shim, M.; Bangsaruntip, S.; Dai, H. J. *J. Am. Chem. Soc.* **2002**, *124* (31), 9058–9059.
(16) Day, T. M.; Unwin, P. R.; Wilson, N. R.; Macpherson, J. V. *J. Am. Chem. Soc.* **2005**, *127* (30), 10639–10647.
(17) Loffler, M. S.; Gross, B.; Natter, H.; Hempelmann, R.; Krajewski, T.; Divisek, J. *Phys. Chem. Chem. Phys.* **2001**, *3* (3), 333–336.
(18) Natter, H.; Hempelmann, R. *Electrochim. Acta* **2003**, *49* (1), 51–61.
(19) He, Z. B.; Chen, J. H.; Liu, D. Y.; Tang, H.; Deng, W.; Kuang, W. F. *Mater. Chem. Phys.* **2004**, *85* (2−3), 396–401.
(20) Yu, J. S.; Kang, S.; Yoon, S. B.; Chai, G. *J. Am. Chem. Soc.* **2002**, *124* (32), 9382–9383.
(21) Terrones, M. *Int. Mater. Rev.* **2004**, *49*, 325–377.
(22) Gooding, J. J. *Electrochim. Acta* **2005**, *50* (15), 3049–3060.

* To whom correspondence should be addressed. Tel: +49-234-3226200. Fax: +49-234-3214683. E-mail: Wolfgang.Schuhmann@rub.de. Web site: www.rub.de/elan.

(1) Reddington, E.; Sapienza, A.; Gurau, B.; Viswanathan, R.; Sarangapani, S.; Smotkin, E. S.; Mallouk, T. E. *Science* **1998**, *280* (5370), 1735–1737.
(2) Carrette, L.; Friedrich, K. A.; Stimming, U. *ChemPhysChem* **2000**, *1* (4), 162–193.
(3) Chen, G. Y.; Delafuente, D. A.; Sarangapani, S.; Mallouk, T. E. *Catal. Today* **2001**, *67* (4), 341–355.
(4) Reetz, M. T. *Angew. Chem., Int. Ed.* **2002**, *41* (8), 1335–1338.

plication.[25] Their incorporation as catalyst support can improve the dispersion of catalysts, thus the productive use of the loaded catalysts.[26]

A variety of techniques is available for the investigation of the electrochemical properties of catalyst materials. Among these, scanning electrochemical microscopy (SECM) with its different modes of operation such as the feedback mode[27] and the tip generation-sample collection (TG-SC) mode[28−31] has proven its applicability in the investigation of the properties of electrocatalysts. However, a major drawback of the TG-SC mode is the large background signal from the measured substrate, which limits the resolution.[32,33] In order to overcome the resolution limitation within the TG-SC mode and to avoid the depletion of oxygen in the gap between tip and sample, the redox-competition mode of SECM (RC-SECM) was developed[33,34] with a special focus on the oxygen reduction reaction (ORR). In this mode, a pulse potential is applied to the SECM tip at each point of the scanning grid. In the first step, oxygen is generated at the tip by anodic water splitting. Subsequently, the potential of the tip is switched to a value at which oxygen reduction is initiated. During this step, the sample and the tip compete for the very same produced oxygen in the gap between tip and sample depending on the applied potential as well as the electrocatalytic activity of the sample. The current flowing through the SECM tip, thus, reflects the activity of the perpendicularly located sample surface, which locally alters the oxygen concentration depending on its activity. In this way, the activity of the sample can be visualized. By carefully adjusting the potential of the sample, it is possible to compare different catalyst materials on a semiquantitative basis.

The aim of this contribution is to present a comparatively fast and semiquantiative method for the investigation of electrodeposited electrocatalysts. In this method, a capillary-based droplet-cell[35−39] is used as a tool to electrodeposit a series of spots of catalyst candidates on glassy carbon modified with CNTs. The catalyst spots are investigated with respect to their electrocatalytic activity for the oxygen reduction as a test reaction on a qualitative and a semiquantitative basis employing RC-SECM.

(23) Dyke, C. A.; Tour, J. M. *J. Phys. Chem. A* **2004**, *108* (51), 11151–11159.
(24) Serp, P.; Corrias, M.; Kalck, P. *Appl. Catal., A* **2003**, *253*, 337–358.
(25) Xia, W.; Su, D. S.; Birkner, A.; Ruppel, L.; Wang, Y. M.; Woll, C.; Qian, J.; Liang, C. H.; Marginean, G.; Brandl, W.; Muhler, M. *Chem. Mater.* **2005**, *17* (23), 5737–5742.
(26) Chen, X. X.; Li, N.; Eckhard, K.; Stoica, L.; Xia, W.; Assmann, J.; Muhler, M.; Schuhmann, W. *Electrochem. Commun.* **2007**, *9* (6), 1348–1354.
(27) Liu, B.; Bard, A. J. *J. Phys. Chem. B* **2002**, *106* (49), 12801–12806.
(28) Fernandez, J. L.; Bard, A. J. *Anal. Chem.* **2003**, *75* (13), 2967–2974.
(29) Walsh, D. A.; Fernandez, J. L.; Bard, A. J. *J. Electrochem. Soc.* **2006**, *153* (6), e99−e103.
(30) Fernandez, J. L.; Walsh, D. A.; Bard, A. J. *J. Am. Chem. Soc.* **2005**, *127* (1), 357–365.
(31) Fernandez, J. L.; White, J. M.; Sun, Y.; Tang, W.; Henkelman, G.; Bard, A. J. *Langmuir* **2006**, *22* (25), 10426–10431.
(32) Fernandez, J. L.; Bard, A. J. *Anal. Chem.* **2003**, *75* (13), 2967–2974.
(33) Eckhard, K.; Chen, X. X.; Turcu, F.; Schuhmann, W. *Phys. Chem. Chem. Phys.* **2006**, *8* (45), 5359–5365.
(34) Eckhard, K.; Schuhmann, W. *Electrochim. Acta* **2007**, *53* (3), 1164–1169.
(35) Lohrengel, M. M.; Rosenkranz, C.; Kluppel, I.; Moehring, A.; Bettermann, H.; Van den Bossche, B.; Deconinck, J. *Electrochim. Acta* **2004**, *49* (17−18), 2863–2870.
(36) Hassel, A. W.; Seo, M. *Electrochim. Acta* **1999**, *44* (21−22), 3769–3777.
(37) Krawiec, H.; Vignal, V.; Oltra, R. *Electrochem. Commun.* **2004**, *6* (7), 655–660.
(38) Eng, L.; Wirth, E.; Suter, T.; Bohni, H. *Electrochim. Acta* **1998**, *43* (19−20), 3029–3033.
(39) Suter, T.; Bohni, H. *Electrochim. Acta* **1997**, *42* (20−22), 3275–3280.

EXPERIMENTAL SECTION

Chemicals and Solution Preparation. $H_2PtCl_6 \cdot 6\ H_2O$, $HAuCl_4 \cdot 3H_2O$, $RhCl_3 \cdot H_2O$ (ca. 38% Rh in weight) were purchased from Acros Organics, Belgium. $RuCl_3 \cdot H_2O$ (ca. 41% Ru in weight) was bought from Sigma-Aldrich, Germany. Glycerol and H_3PO_4 (85%) were obtained from J.T.Baker, The Netherlands; KH_2PO_4 was obtained from VWR, Germany, and $K_2HPO_4 \cdot 3H_2O$ from Merck, Germany.

For the electrodeposition, aqueous solutions with concentrations of 1 mM (for qualitative SECM studies), 2.5, 5, and 10 mM (for semiquantitative SECM studies) of the metal salts (either single or as a mixture of two metal salts) were prepared using deionized tridistilled water, followed by adding 4.6 g of glycerol into 2.5 mL of the aqueous solution to obtain a highly viscous solution. Phosphate buffer (0.1 M, pH = 6.7) was prepared by mixing 0.1 M KH_2PO_4 and 0.1 M $K_2HPO_4 \cdot 3H_2O$ in a volume ratio of 1:1. Phosphate buffer with a pH value of 2.84 was prepared by mixing H_3PO_4 and KH_2PO_4.

Modification of SECM Substrate with Carbon Nanotubes. Carbon nanotubes (CNTs) (Pyrograf III, pyrolytically stripped, diameter: 100−200 nm, length: 30−100 μm, Applied Sciences, Buffalo, NY) were treated with concentrated HNO_3 at 120 °C for about 90 min. After filtration, the CNTs were washed with distilled water in order to completely remove the acid. The acid pretreated CNTs were then dispersed into deionized tridistilled water in an ultrasonic bath to prepare an aqueous suspension of CNTs with a loading of 0.2 mg mL^{-1}. The glassy carbon (GC) plates (SigradurG, HTW Hochtemperatur-Werkstoffe, Germany), which were used as the SECM substrate, were polished on a polishing cloth with diamond (6 and 3 μm) and alumina paste (1 and 0.3 μm) (Leco, St Joseph, MI) before being modified with CNTs. A DC power supply (Voltcraft, Germany) was used for the electrophoretic accumulation of acid pretreated CNTs on the GC surface. The target GC was connected as the positive pole whereas another GC plate of similar size was used as the negative pole. A potential of 10 V was applied for 10 s for electrophoretic accumulation of CNTs.
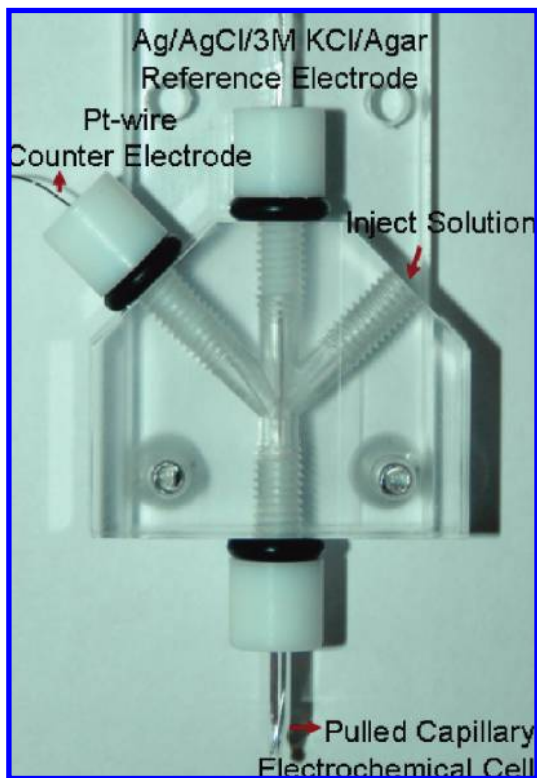
Capillary-Based Droplet-Cell for Preparing Catalyst Spots. Catalyst spots modified with Pt, Ru, Rh, Au, and their codeposits were prepared on CNTs-modified GC by means of pulsed electrodeposition using a capillary-based droplet-cell (Figure 1). A borosilicate capillary (outer diameter: 2.5 mm, wall thickness: 0.25 mm, obtained from Hilgenberg, Germany) was pulled with a capillary puller to diameters <500 μm to constitute the electrochemical cell. During electrodeposition, its small tip touches the CNTs/GC surface. A Ag/AgCl/3 M KCl/agar gel electrode sealed in a glass capillary as described by Hassel et al.[40] and a Pt-wire were used as reference and counter electrode, respectively. The CNTs/GC substrate was connected as the working electrode to complete the electrochemical circuit. The droplet-cell was fixed to a stepper-motor so that a well-defined array of catalyst spots could be prepared.

A potentiostat/galvanostat (PG 310, HEKA, Germany) was employed for the direct electrodeposition of metal particles. In a first series of experiments, a pulse potential profile of 200 mV (500 ms) ∼ −1200 mV (100 ms) ∼ 200 mV (500 ms) (vs Ag/

(40) Hassel, A. W.; Fushimi, K.; Seo, M. *Electrochem. Commun.* **1999**, *1* (5), 180–183.

Figure 1. Capillary-based droplet-cell with a Pt-wire as counter electrode, a Ag/AgCl/3 M KCl/agar as the reference electrode and a pulled borosilicate capillary as the electrochemical cell.

AgCl/3 M KCl/agar) was applied and 30 pulses were used for each deposition. In this way, a rather high loading of small metal particles on the nanotubes could be achieved. However, this approach was not suitable for a semiquantitative assessment of the catalyst activity. For this purpose, a pulse potential profile of −800 mV (500 ms) ∼ 600 mV (500 ms), using only a single pulse, was applied. After electrodeposition from the viscous solution, the catalyst/CNTs/GC substrate was immersed into deionized tridistilled water and moved gently so that potentially adhering glycerol and residual metal ions could be removed completely.

SECM Instrumentation and Measurement. A 4-electrode SECM setup combined with a bipotentiostat (Jaissle PG100, Germany)[33,34] was used to visualize the electrocatalytic activity toward the ORR of the prepared catalyst spots. A Ag/AgCl/3 M KCl double junction electrode and a Pt foil were used as the reference electrode and counter electrode, respectively. The sample (catalyst/CNTs/GC) was used as one working electrode while a Pt disk electrode with diameter of 25 μm (for the qualitative study) or 50 μm (for the semiquantitative study) was used as SECM tip, i.e., the second working electrode. The tip to sample distance was set to 80% of the measured current with respect to the bulk current by performing a feedback approach curve, using molecular oxygen as free-diffusing redox mediator. For the redox-competition mode of SECM, the following potential pulse profile was used: 500 mV (base potential, 0.2 s) ∼ 1200 mV (anodic water splitting, 0.2 s) ∼ −600 mV (oxygen competition, 0.3 s), all potentials vs Ag/AgCl/3 M KCl. For the qualitative evaluation of electrocatalytic activity, the sample was polarized to different potentials (−150, −200, −300, −450, and −600 mV) to distinguish the electrocatalytic activity toward the ORR in phos-

phate buffer (pH = 6.7) by means of the onset of activity. For the semiquantitative assessment of activity, the sample was polarized to a potential of −600 mV.

RESULTS AND DISCUSSION

Electrophoretic Accumulation of Carbon Nanotubes onto Glassy Carbon. Glassy carbon (GC) with a smooth surface is frequently used as substrate for SECM experiments. However, with the aim of extending the applicability of the SECM technique to porous, 3-dimensional surfaces, we have modified the GC substrate with CNTs. CNT-modified surfaces additionally represent a more realistic model, e.g., of fuel cell electrodes. Moreover, due to the increased surface area, higher catalyst loadings can be achieved without extensive nanoparticle agglomeration. It was previously reported that CNTs can be fixed to supporting materials such as carbon fibers[41] or glassy carbon[42] by directly dropping a dispersion of CNTs containing Nafion as a binder onto the surface. However, the incorporation of Nafion will result in problems during the subsequent electrochemical analysis.[26] The homogeneity of the dispersed CNTs on the surface obtained by a simple dropping procedure will strongly depend on both the dispersion of CNTs in the suspension and their adhesion to the underlying supports. With the need of a rather homogeneous surface for further SECM studies, a simple method to deposit CNTs onto the GC surface by means of electrophoretic accumulation[43,44] was applied. The amount of CNTs accumulated on the GC surface can be varied by adjusting different parameters (Figure 2), such as the amount of CNTs in the suspension or the voltage and duration for the electrophoretic accumulation. In case of accumulating a higher amount of the hydrophilic CNTs on the GC surface, the electrolyte inside the capillary forming the droplet-cell may be sucked out upon touching the CNTs/GC surface during catalyst deposition (Figure 2A). In order to prevent this, the amount of CNTs in the suspension was adjusted to 0.2 mg mL⁻¹ (Figure 2B). Using these conditions, the CNTs are still homogeneously spread over the GC surface. It is important to note that the accumulated CNTs remain attached to the GC surface even during long-term experiments in phosphate buffer (at least 2 days), which is considered to be an important prerequisite for the envisaged reliable SECM screening.

Electrodeposition of Catalyst Spots Using the Droplet-Cell. The capillary-based droplet-cell described in the Experimental Section has been used to prepare arrays of catalyst spots by either varying the nature of the active metal or the composition of metals. These metal deposits on CNTs are then further investigated with regard to their electrocatalytic activity by means of SECM. For the first experiments, the tip of the droplet-cell was modified by a silicon ring[35,45,46] with the purpose of preventing leakage from the tip. Catalyst spots with the size defined by the diameter of

(41) Qing, W. X.; Liu, X. H.; Lu, H. M.; Liang, J.; Liu, K. Z. *Microchim. Acta* **2008**, *160* (1−2), 227−231.
(42) Musameh, M.; Lawrence, N. S.; Wang, J. *Electrochem. Commun.* **2005**, *7* (1), 14−18.
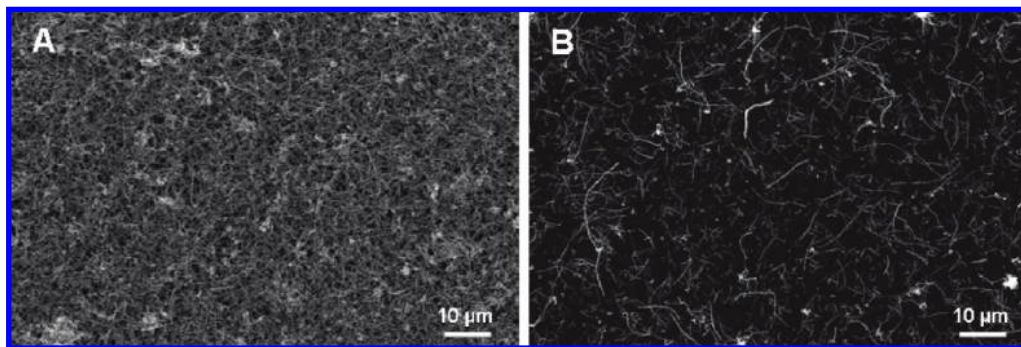(43) Valentini, F.; Palleschi, G.; Morales, E. L.; Orlanducci, S.; Tamburri, E.; Terranova, M. L. *Electroanalysis* **2007**, *19* (7−8), 859−869.
(44) Valentini, F.; Orlanducci, S.; Terranova, M. L.; Palleschi, G. *Sens. Actuators, B* **2007**, *b123* (1), 5−9.
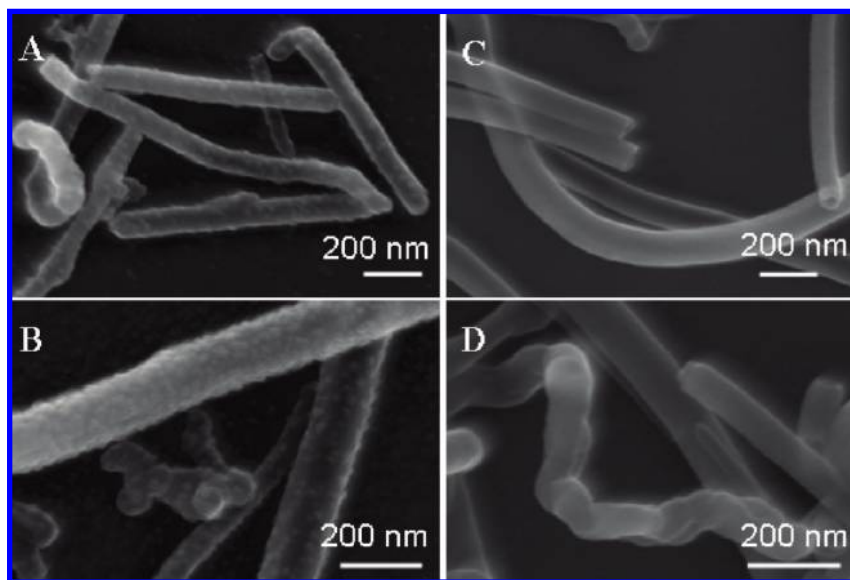(45) Suter, T.; Bohni, H. *Electrochim. Acta* **2001**, *47* (1−2), 191−199.
(46) Lohrengel, M. M.; Moehring, A.; Pilaski, M. *Electrochim. Acta* **2001**, *47* (1−2), 137−141.

Figure 2. Glassy carbon surfaces modified with CNTs via electrophoretic deposition. Aqueous suspensions of (A) 1 mg/mL CNTs and (B) 0.2 mg/mL CNTs were used for CNT deposition on GC plates (10 V for ca. 10 s).

Figure 3. SEM images of (A) Pt, (B) Au, (C) Ru, and (D) Rh electrodeposited onto CNTs/GC. The electrodeposition was performed from an aqueous solution of the metal ion (1 mM) containing 1.84 g mL^{-1} glycerol by applying 30 pulses with a pulse potential profile of 200 mV (500 ms) $\sim$ −1200 mV (100 ms) $\sim$ 200 mV (500 ms) (vs Ag/AgCl/3 M KCl/agar).

the capillary forming the droplet-cell were fabricated also using an unmodified tip without leakage of solution during the pulsed electrodeposition if smaller amounts of the hydrophilic CNTs were accumulated on the GC surface.

It has recently been shown that introduction of a viscous additive to an aqueous metal ion containing solution can severely slow down the diffusional mass transport of metal ions, thus limiting the growth of electrodeposited metal nanoparticles.[26] This approach has been adopted to be used in the droplet-cell in the present study. Figure 3 shows scanning electron microscopy (SEM) images of different single metal deposits on CNTs/GC, which were prepared using the capillary-based droplet-cell by pulsed electrodeposition in diffusion-restricted solutions. Deposited Au (Figure 3B) shows a higher particle density and bigger particle sizes as compared to the other metals (Figure 3A,C,D) when the same deposition parameters were applied. This is of course due to the different reduction potentials of the deposited metals. The size of the nanoparticles was for all cases about 20 nm or smaller even when 30 deposition pulses were applied for the pulsed electrodeposition. Although Ru and Rh nanoparticles can hardly be seen in the SEM images, the below described

evaluation of the catalytic activity definitely proved that both metals were successfully electrodeposited on top of the CNTs-modified GC surface.

Visualization of the Electrocatalytic Activity of Metal Deposits by Means of the Redox-Competition Mode of SECM. The electrodeposited metal catalyst spots were investigated using the redox-competition mode of SECM (RC-SECM) for visualization of their electrocatalytic activity toward the ORR in a 0.1 M phosphate buffer (pH 6.7). Figure 4 shows SECM images obtained upon screening of spots of different single metal catalysts (Pt, Au, Ru, Rh) (Figure 4A) and spots of mixed Au−Pt deposits (Figure 4B). The sample was polarized to different potentials to distinguish the onset potential, which can be used as a measure for activity for the ORR for the different catalyst spots. The onset potential here is defined as the potential, where the local catalytic activity for the ORR can be clearly visualized with RC-SECM. Due to the experimental approach as well as the fact that larger increments in potential changes were used, this might not reflect the values obtained by other methods; however, it will give a reliable order of activity of the different deposits. When the SECM tip is located above an oxygen consuming site, the local amount of oxygen is decreased, concomitantly decreasing the current detected by the
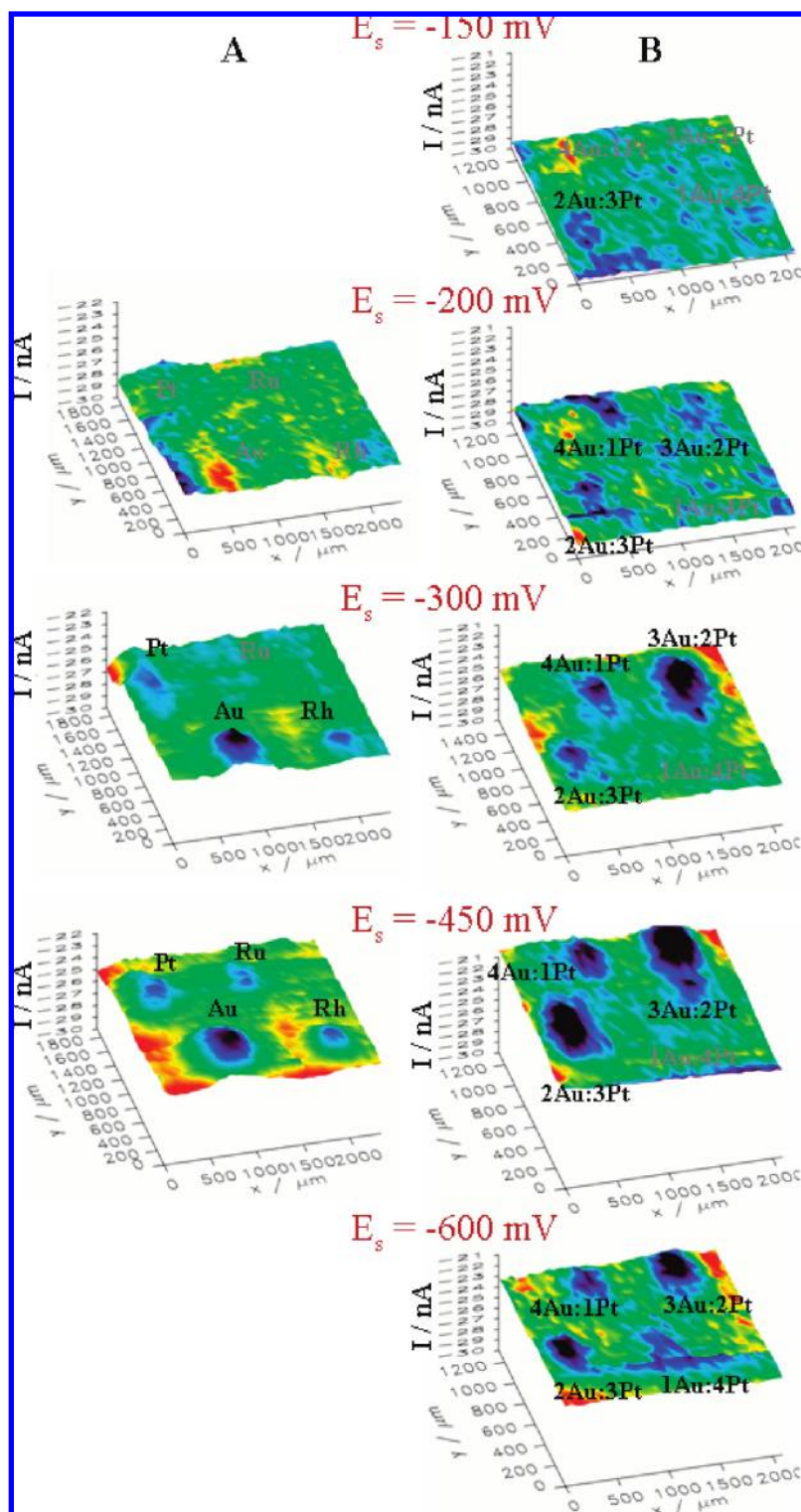
Figure 4. Redox-competition SECM images of oxygen reduction activity in 0.1 M phosphate buffer (pH 6.7) measured at various sample potentials on (A) single metal catalysts (Pt, Au, Ru, Rh) and (B) coelectrodeposited Au−Pt catalysts electrodeposited from solutions with different initial Au^{3+}/Pt^{4+} ratios (4:1, 3:2, 2:3, and 1:4). Grid increment: 50 × 50 μm.

SECM tip. The higher the local catalytic activity toward the ORR, the less negative is the detected oxygen reduction current at the SECM tip.[33] For the spots of single metal catalysts (Figure 4A), the SECM image exhibits a flat current surface at $E_s = -200$ mV demonstrating that the electrocatalytic activity of the catalysts toward the ORR is negligible. Au as well as Pt and Rh exhibit activity toward the ORR in phosphate buffer when

a potential of −300 mV is applied to the sample. At $E_s = -450$ mV, Ru finally starts to show electrocatalytic activity toward the ORR. In this specific case, Au exhibits the highest electrocatalytic activity for oxygen reduction among all studied single metal catalysts. The reason for this is most probably seen in a much higher loading of Au, as suggested by the SEM image in Figure 3. By coelectrodeposition of Au−Pt mixtures

Table 1. Onset Potentials for the ORR (i.e., Potential at Which ORR in RC-SECM Experiments Becomes Visible) Over Ru–Pt and Rh–Pt Mixtures in 0.1 M Phosphate Buffer (pH 6.7)[a]

	4Ru:1Pt	3Ru:2Pt	2Ru:3Pt	1Ru:4Pt	4Rh:1Pt	3Rh:2Pt	2Rh:3Pt	1Rh:4Pt
E_s (mV)	−450	−450	−300	−200	−450	−300	−450	−300

[a] The composition is given as the molar ratio of metal ions in the solution for the pulsed electrodeposition.

Table 2. Calculation of the Catalyst Loading Based on the Transferred Charge during the Pulsed Electrodeposition

	charge (Q) during pulsed electrodeposition (μC)	absolute charge (Q) after subtracting blank solution (μC)	electron transferred ($n = q/F^a$) (pmol)	catalyst loading ($n/3^b$) (pmol)
blank	0.176			
Ru 10	1.342	1.166	12.084	4.0281
Ru 5	0.743	0.5670	5.8763	1.9588
Ru 2.5	0.552	0.376	3.8968	1.2989
Au 2.5	1.085	0.909	9.4207	3.1402
Au 5	1.675	1.499	15.535	5.1784
Au 10	2.975	2.799	29.01	9.6694

[a] F (Faraday constant) = 96 490 C mol^{-1}. [b] 1 mol catalyst electrodeposited will need 3 mol electrons transferred (Ru^{3+} to Ru and Au^{3+} to Au).

(Figure 4B), electrocatalytic activity toward the ORR in phosphate buffer is obtained at a less negative sample potential ($E_s = -150$ mV). At $E_s = -150$ mV, Au–Pt electrodeposited from a solution with a Au/Pt molar ratio of 2:3 in the deposition solution shows the most positive onset potential in SECM investigations. Catalysts deposited from solutions with molar ratios of the metal ions such as 4:1 and 3:2 started to show the electrocatalytic activity toward the ORR at $E_s = -200$ mV. The sample with a molar ratio of metal ions of 1:4 showed activity toward the ORR only at $E_s = -600$ mV.

RC-SECM experiments were also carried out over Ru–Pt and Rh–Pt codeposited catalysts (SECM images not shown). Table 1 summarizes the potentials at which the ORR was detected over Ru–Pt and Rh–Pt catalyst spots. Combining the information of both Figure 4 and Table 1, it becomes evident that most of the Au–Pt mixtures showed significant improvements for the ORR in phosphate buffer, as compared with the single metals, which is demonstrated by a more positive potential at which the ORR was detected. In addition, these codeposits also exhibit electrocatalytic activity toward the ORR at more positive potentials (e.g., $E_s = -150$ and -200 mV) than Ru–Pt and Rh–Pt mixtures (e.g., $E_s = -300$ and -450 mV). Although the single Ru metal deposit exhibited activity at a more negative potential ($E_s = -450$ mV), the electrocatalytic activity toward the ORR was improved upon codeposition with Pt (e.g., $E_s = -200$ and -300 mV). Ru–Pt with a molar ratio of the metal ions of 1:4 in the deposition solution started to show electrocatalytic activity toward the ORR at an even more positive potential ($E_s = -200$ mV) than Pt alone ($E_s = -300$ mV).

Semi-Quantitative Evaluation of the Electrocatalytic Activity of Different Metal Catalysts toward the ORR. The above results clearly demonstrate that RC-SECM presents a tool to evaluate the local electrocatalytic activity toward the ORR of arrays of catalyst spots, even if more complex sample surfaces like CNTs/GC were used. However, in order to use SECM in a combinatorial approach for the screening of new materials, at least a semiquantitative assessment of catalytic activity is required. For instance, Pt, which is known to be the most active single metal for catalyzing the ORR has shown a weaker electrocatalytic activity

toward the ORR in phosphate buffer (pH 6.7) than Au at the same sample potential (Figure 4A). Obviously, the electrocatalytic activity is, besides being influenced from, e.g., the pH of the solution, affected by many factors, such as size and shape of the catalyst nanoparticles and the active surface area, as well as the loading of catalysts. Hence, the evaluation of the real electrocatalytic activity of different catalyst materials by SECM is a big challenge. In this regard, controlling the shape and size of different catalyst materials prepared by electrodeposition as well as determining the active surface area of the obtained metal nanocluster deposits is extremely difficult.

Therefore, for the semiquantitative investigation of catalytic activity, we have focused on the loading, i.e., the amount of deposited material, which is, at least from the point of view of possible applications in industry, a very important quantity. As examples, we have chosen the two materials which exhibited the highest and the lowest activity in our previous experiments, i.e., Au and Ru, respectively. For the determination of the loading, the charge used for electrodeposition was taken. From the measured charge, the blank charge, which is caused by capacitive effects, had to be subtracted, which has been determined in a control experiment in phosphate buffer at a similar pH-value (pH = 2.84) as the one of the aqueous solutions of metal ions (pH = 2.78–3.35) containing an identical amount of glycerol (1.84 g mL^{-1}).

A potential step profile of -800 mV (0.5 s) ~ 600 mV (0.5 s) with only a single pulse was applied to prepare Au and Ru spots on a CNTs/GC surface using the capillary-based droplet-cell. The reason to use a single pulse only was that, as soon as catalyst particles are formed, the ORR at these particles may contribute to the charge measured, causing an unpredictable error in the calculation of the loading. The charge of the fraction of oxygen, which is reduced at the glassy carbon during the pulse and, thus, contributed to the overall charge, will be eliminated by subtracting the blank charge. To work under oxygen-free conditions, the use of the droplet-cell is not possible to overcome this problem. The same pulse time of 500 ms for both -800 and 600 mV was chosen with the purpose of minimizing the effect from double layer charging. The spots were prepared from solutions with different
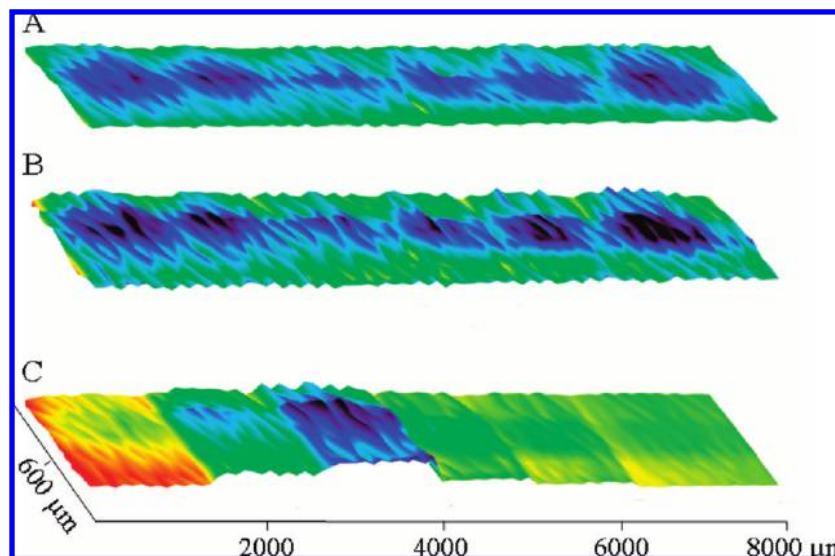
Figure 5. (A) SECM image of oxygen reduction activity on different catalyst spots (from left to right: Ru electrodeposited from 10, 5, and 2.5 mM RuCl₃/glycerol solution containing 1.84 g/mL glycerol; Au electrodeposited from 2.5, 5, and 10 mM HAuCl₄/glycerol solution containing 1.84 g/mL glycerol) in phosphate buffer (pH 6.7) at $E_s = -600$ mV; (B) corrected SECM image after subtracting the background from the initial SECM image; (C) normalized SECM image after dividing the absolute current at each grid point of the individual spots and its surrounding area by the total catalyst loading of the spot, which was derived from the charge transferred during electrodeposition.

initial concentrations (10, 5, and 2.5 mM) of the metal ions containing 1.84 g mL⁻¹ glycerol. Table 2 summarizes the charge and catalyst loading for Au and Ru deposited from solutions with various metal ion concentrations. As seen in Table 2, the catalyst loading at each spot can be finally calculated on the basis of the transferred charge during the reaction. With the increase of the initial concentration of metal ions in solution, the amount of electrodeposited catalyst on the CNTs/GC surface increased when the same deposition parameters were applied.

RC-SECM measurements were carried out over Ru and Au spots with different loadings as calculated in Table 2 (Figure 5A). A 50 μm Pt-disk electrode was used to scan over the sample with an increment of 100 μm in the X-direction and 150 μm in the Y-direction. Nine lines were scanned in the X-direction in order to scan across the entire spots. The CNTs/GC surface modified with six different catalyst spots was polarized at −600 mV, a potential at which both Ru and Au showed electrocatalytic activity toward the ORR in phosphate buffer (pH 6.7) in the above-described qualitative experiments. For semiquantitative evaluation of the electrocatalytic activity of the different catalyst spots, the background current along each scan in the X-direction was subtracted from the detected current at each point of the scanning grid in the same scan. Figure 5B shows the corrected SECM image after subtracting the background current from the initial SECM image. As expected, all six catalyst spots exhibit electrocatalytic activity toward the ORR at $E_s = -600$ mV. The spots with a higher loading of the same catalyst (the left Ru spot and the right Au spot) showed a higher electrocatalytic activity, which is clearly demonstrated by a stronger contrast in the SECM image. After normalizing the SECM image by the loading of the metal catalysts as derived from the charge during spot formation, a SECM image with semiquantitative information concerning the electrocatalytic activity toward the ORR in phosphate buffer over the different catalyst spots was obtained (Figure 5C). The image was obtained by dividing the measured current corrected by the background current as shown in Figure

5B of an individual spot and its surrounding area by the catalyst loading of the spot, which was obtained from the transferred charge during electrodeposition. In contrast to the observation from Figure 5B, the Ru spot with the lowest loading exhibited the highest mass specific electrocatalytic activity, which is likely due to the deposition of smaller particles from the lower Ru ion concentration. In addition, all Ru spots showed higher electrocatalytic activities toward ORR than the Au spots irrespective of their loading.

CONCLUSION

Pulsed electrodeposition in a diffusion-restricted viscous solution has been used to deposit well-dispersed catalyst nanoparticles onto CNTs-modified GC. Electrophoretic accumulation of CNTs on GC proved to be a simple method to prepare CNTs/GC substrates, which may serve as model substrates for further electrocatalysis studies. A capillary-based droplet-cell has been used to deposit arrays of catalyst spots onto these substrates, which can then be investigated by the redox-competition mode of the SECM with regard to their electrocatalytic activity for oxygen reduction in a single experiment. A semiquantitative comparison of the activity of the deposited metal catalysts can be achieved by monitoring the charge used for electrodeposition and normalizing the activity by the metal loading.